









## Bio-Based Modification of Natural Rubber-Modified Asphalt Using Hard Resin from Yang

Poramin Sinthorn<sup>1</sup>, Supakorn Tirapat<sup>1\*</sup>, Somporn Katekaew<sup>2</sup>, Ampol Wongsas<sup>1</sup>,  
Patcharapol Posi<sup>3</sup>, Chanachai Thongchom<sup>4</sup>, Prinya Chindaprasirt<sup>1</sup>

<sup>1</sup> Department of Civil Engineering, Faculty of Engineering, Khon Kaen University, Khon Kaen, 40002, Thailand.

<sup>2</sup> Department of Biochemistry, Faculty of Science, Khon Kaen University, Khon Kaen 40002, Thailand.

<sup>3</sup> Department of Civil Engineering, Faculty of Engineering, Rajamangala University of Technology Isan, Khon Kaen Campus, Khon Kaen 40000, Thailand.

<sup>4</sup> Thammasat University Research Unit in Structural and Foundation Engineering, Department of Civil Engineering, Thammasat School of Engineering, Thammasat University, Klongluang, Pathumthani 12120, Thailand.

Received 18 June 2025; Revised 09 October 2025; Accepted 12 October 2025; Published 01 November 2025

### Abstract

This study investigates the potential of hard resin derived from the Yang tree (HY), a renewable bio-based byproduct, as a performance-enhancing additive in natural rubber-modified asphalt (NRMA). HY-modified binders (HYMA) containing 3%, 7%, and 15% HY by weight were evaluated through a multi-scale experimental program, including physical, rheological, thermal, chemical, and mechanical tests. Standard binder characterizations (penetration, ductility, softening point, viscosity), spectroscopic analyses (FT-IR, NMR), microstructural observations (ESEM, XRD), thermal profiling (DSC), and performance assessments (DSR, Marshall) were conducted. The results demonstrated that HY improved binder properties at optimal concentration by introducing additional hydrocarbon structures without chemical cross-linking. HYMA3 achieved the most favorable balance of stiffness, flexibility, and compaction efficiency, whereas higher HY contents ( $\geq 7\%$ ) impaired structural integrity and deformation resistance. Microstructural and thermal evidence confirmed surface modifications and altered thermal transitions, which influenced viscoelastic response. These findings provide new insights into bio-resin-asphalt interactions and establish the viability of HY as a sustainable alternative to synthetic polymer modifiers. Beyond performance improvement, HY promotes circular construction by transforming agricultural byproducts into functional pavement materials, supporting the development of climate-adaptive infrastructure.

**Keywords:** Yang; Hard Resin; Dipterocarpus Alatus; Natural Rubber-Modified Asphalt; Bio-Based Modifier; Sustainable Pavement Materials.

## 1. Introduction

Flexible pavement remains one of the most widely adopted forms of road infrastructure because of its cost-effectiveness, ease of maintenance, and adaptability to varying traffic and environmental conditions [1]. The performance of its asphalt binder is influenced by physical consistency, chemical composition, thermal and rheological behavior, microstructural uniformity, and mechanical strength [2, 3]. The resistance of the binder to temperature fluctuations, oxidative aging, and repeated traffic loading directly governs pavement rutting resistance, fatigue life, and cracking susceptibility.

\* Corresponding author: [supati@kku.ac.th](mailto:supati@kku.ac.th)



<http://dx.doi.org/10.28991/CEJ-2025-011-11-018>



© 2025 by the authors. Licensee C.E.J, Tehran, Iran. This article is an open access article distributed under the terms and conditions of the Creative Commons Attribution (CC-BY) license (<http://creativecommons.org/licenses/by/4.0/>).

To overcome the inherent limitations of conventional asphalt, a wide range of modifiers has been investigated, including natural and synthetic polymers [4, 5], recycled rubber [6–8], and bio-based additives [9], with the dual objective of improving performance and promoting environmental sustainability [10–12]. Among these, natural rubber (NR) obtained from *Hevea brasiliensis* is widely acknowledged as a renewable, eco-friendly elastomer with outstanding elasticity and fatigue resistance. Due to its abundance in Southeast Asia, NR is considered a cost-effective alternative to synthetic polymers [12–14]. When blended with asphalt to form natural rubber–modified asphalt (NRMA), the flexible polyisoprene chains of NR have been shown to improve rheological, thermal, and mechanical properties, thereby enhancing binder stability [15]. The optimum NR content is typically reported in the range of 4–6 wt.% [14], whereas approximately 7 wt.% has been shown to enhance high-temperature resistance in tropical regions such as Thailand [15, 16]. However, higher NR dosages are frequently associated with poor dispersion, increased processing viscosity, and greater susceptibility to oxidative degradation.

To mitigate these drawbacks, researchers have investigated co-modifiers such as styrene–butadiene–styrene (SBS) [17], cup lump rubber with polyphosphoric acid (PPA) [13, 18], and rejuvenating oils derived from waste or virgin cooking and engine oils [11, 19–21]. In parallel, pyrolysis-derived binders from waste biomass (e.g., wood [22, 23]) and plastics [24, 25] have been explored as sustainable alternatives. More recently, bio-oils obtained from renewable biomass—including forestry residues and agricultural waste—have attracted increasing attention for their ability to improve asphalt binder performance. Vegetable oils such as waste sunflower and rapeseed oil [26], castor oil [27], and lignocellulosic bio-oil [28] have been reported to reduce viscosity and enhance low-temperature performance, while their aromatic-rich structures promote chemical stability. Compared with crumb rubber, which primarily improves high-temperature rheology, bio-oils are particularly effective in enhancing low-temperature flexibility owing to their light molecular fractions [23, 29, 30]. A comparative summary of bio-oils from different sources is presented in Table 1.

**Table 1. Summary of previous studies on the application of bio-oils as asphalt modifiers**

Raw Materials	Performance Highlights	Conclusion	Color	Reference
Sunflower oil, Rapeseed oil	The binder exhibited improved resistance to thermal cracking.	Vegetable oil softens the blend and enhances low-temperature properties.	Light-gold	Some et al. [26]
Castor oil	The binder demonstrated enhanced ductility and improved low-temperature performance.	Bio-oil increases softness and improves low-temperature properties without altering composition.	Dark-brown	Zhang et al. [27]
Castor oil	The material showed increased peak load, fracture displacement, fracture toughness, and fracture energy.	Bio-oil combined with crumb rubber significantly improves resistance to aging and low-temperature cracking.	Dark-brown	Zhou et al. [31]
Castor oil	The binder exhibited high resistance to permanent deformation and thermal cracking.	Asphalt performance decreases when bio-oil is used alone but improves when blended with SBS and crumb rubber.	Dark-brown	Dong et al. [32]
Castor oil	The modified asphalt demonstrated improved low- and high-temperature properties with various ratios of castor oil and PPA.	PPA-modified high-content bio-asphalt exhibits superior performance at both low and high temperatures.	Dark-brown	Ju et al. [33]
Rice straw bio-oil	The material showed high rutting, fatigue, and thermal cracking resistance under different pyrolysis conditions.	Performance depends on pyrolysis temperature, and FTIR confirmed the process as physical fusion.	Dark	Zhou et al. [34]
Plastic pyrolytic oil	The modified binder demonstrated good storage stability and rheological performance.	Storage conditions influence stability and rutting/fatigue resistance in rubberized asphalt.	Dark	Kumar & Choudhary [35]
Wood bio-oil	The binder exhibited high resistance to permanent deformation and fatigue.	Bio-binders are effective and sustainable alternatives to conventional bitumen.	Dark	Ingrassia et al. [22]
Waste wood bio-oil	The binder showed improved resistance to low-temperature cracking.	Bio-oil enhances low-temperature cracking resistance but reduces high-temperature and aging resistance.	Dark	Zhang et al. [23]
Lignocellulose	The modified asphalt demonstrated high thermal stability.	Bio-oil significantly reduces asphalt viscosity, complex modulus, and rutting index.	Dark	Ding et al. [28]

While extensive research has focused on bio-oils, natural resins have received comparatively little attention in pavement engineering. Of particular relevance is the hard resin obtained from the Yang tree (*Dipterocarpus alatus*), a species indigenous to Southeast Asia. Refining of Yang oleoresin yields two primary products as shown in Figure 1: approximately 60–70% Gurjun oil, commonly used as a fuel or in cosmetics, and about 30% by weight of hard resin (HY). HY is dark brown in color as presented in Figure 2 and exhibits moderate viscosity. It also contains a high proportion of hydrocarbons, including oxygenated and carbonyl functional groups [36–38]. Such attributes indicate that HY has the potential to enhance compatibility, stability, and cohesion in asphalt binders, similar to other distilled bio-oils. Although HY has been investigated in biofuel production [36–41] and pharmaceutical applications [42, 43], its potential in asphalt modification—particularly in synergy with natural rubber (NR)—remains largely unexplored. Given its asphalt-like properties, HY represents both opportunities and challenges as a potential partial substitute for conventional asphalt cement, thereby warranting systematic evaluation.

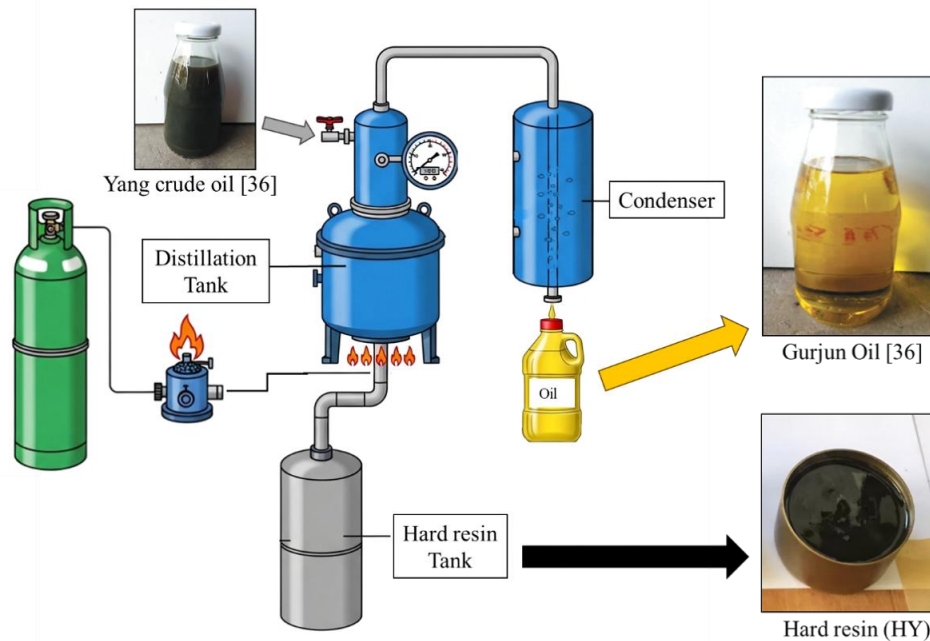


Figure 1. Distillation process of Yang crude oil, producing Gurjun oil and hard resin (HY)

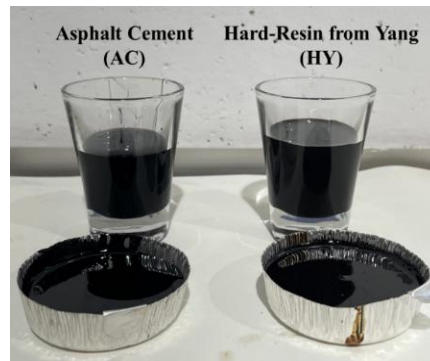


Figure 2. Asphalt cement (AC) and hard-resin from Yang (HY)

This study aims to address this gap by systematically evaluating hard resin from Yang (HY) as a bio-based co-modifier for natural rubber-modified asphalt (NRMA). HY was incorporated at 3%, 7%, and 15% by weight, selected based on reported optimum NR dosages [14–16] and to investigate the effects of higher loadings. A comprehensive experimental program was conducted to examine physical properties (penetration, ductility, softening point, viscosity); chemical composition and molecular interactions (FTIR, NMR); thermal transitions (DSC); rheological behavior (rutting resistance); and microstructural characteristics (ESEM, XRD). Mechanical performance and deformation resistance were further assessed using Marshall stability and flow tests to simulate field-relevant conditions.

The central hypothesis is that HY enhances stiffness, compatibility, and thermal resilience in NRMA while preserving structural integrity and avoiding undesirable cross-linking. By incorporating HY into NRMA, this study seeks to advance the development of high-performance, sustainable asphalt binders and valorize an underutilized local bio-resource for sustainable pavement engineering applications.

## 2. Materials and Methods

### 2.1. Materials

The primary materials used in this study were original asphalt cement (AC), obtained from the Department of Civil Engineering, Khon Kaen University, and hard resin from Yang (HY), derived from the Yang distillation system at the Yang Na Integrated Learning Center, Khon Kaen University. The distillation process is illustrated in Figure 1 and has been described in detail in a previous publication [36]. A comparison of the colors of AC and HY is presented in Figure 2, showing similarly dark to dark-brown tones. The essential properties of both materials, summarized in Table 2, conform to the TIS 851-2018 standard [44]. Following the guidelines in DH-SP 409-2013 [45], the bio-based oil obtained from the distillation process was blended with the original AC binder to produce natural rubber-modified asphalt (NRMA) at three different proportions by weight—3%, 7%, and 15%—designated as HYMA3, HYMA7, and HYMA15, respectively. These proportions were selected based on previous studies on modified asphalt [14–16]. The production process involved heating both AC and HY to 120 °C until liquefied, followed by pouring the molten mixture

into a mold. Blending was carried out for 20 minutes at the same temperature to ensure complete homogenization. A comparison of viscosity data, presented in Figure 3, confirms that under these conditions, the viscosity values of the materials were comparable.

**Table 2. Basic properties of AC and HY**

Properties	AC	HY
Penetration (0.1 mm)	98	127
Ductility (cm)	>100	40
Softening point (°C)	47	41

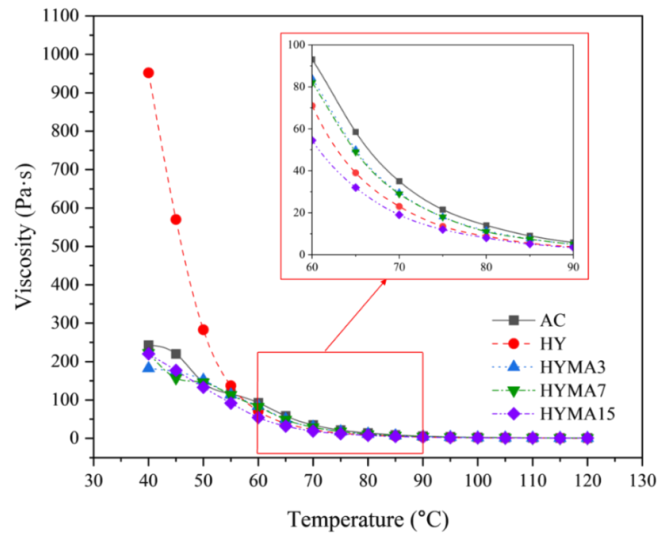


**Figure 3. Relationship between viscosity and temperature**

## 2.2. Experimental Design

A comprehensive laboratory program was conducted to investigate the physical and chemical properties of asphalt cement (AC), hard resin from Yang (HY), and HY-modified asphalt (HYMA), together with the mechanical performance of asphalt concrete incorporating these binders. The overall experimental framework is illustrated in the flowchart shown in Figure 4.

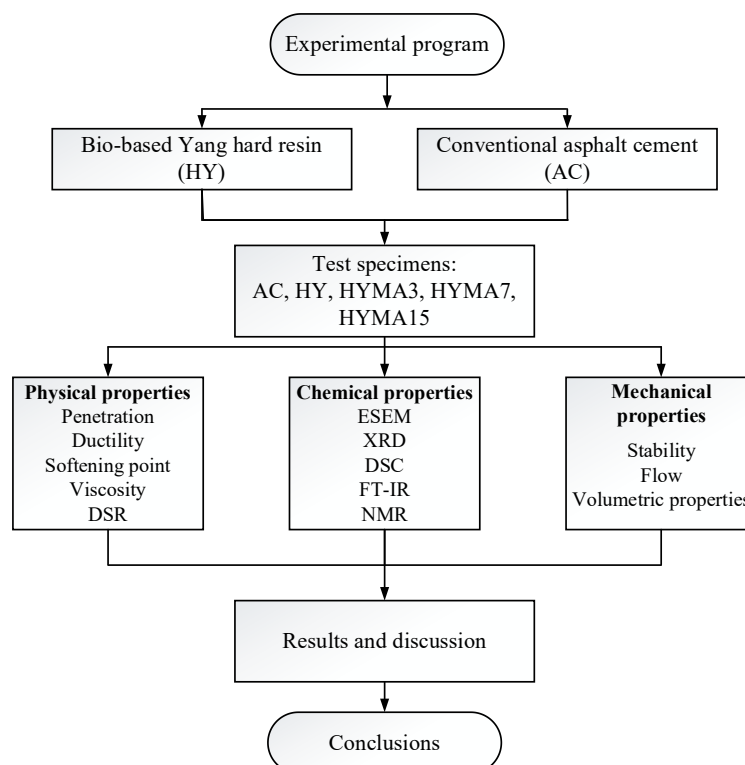


**Figure 4. Research methodology process**

### 2.2.1. Physical Properties

This study presents a comprehensive evaluation of the fundamental physical properties of asphalt binders, highlighting their importance throughout asphalt production, manufacturing, transportation, and pavement construction [11, 14]. These properties are critical for grading, pumping, mixing, and for ensuring optimum asphalt performance under service conditions. Details of each test are presented in the following subsections.

- Penetration Test: Conducted to ascertain the penetration grade and assess asphalt binder quality. This test, aligned with ASTM D5/D5M-13 [46], examines asphalt bitumen consistency under specific loading, duration, and temperature conditions.
- Ductility Test: According to ASTM D113-17 [47], this test explores the tensile characteristics of asphalt bitumen by measuring the elongation of bitumen before breaking at a specific temperature.
- Softening Point Test: Conducted using a ring-and-ball apparatus following ASTM D36-06 [48], this test measures the softening point of bitumen, providing an indication of its viscosity and transition from a solid to a more fluid state.
- Viscosity Test: The apparent viscosity of asphalt at high temperatures is determined by using a rotational viscometer, specifically Malvern Kinexus Ultra Plus Instruments. The torque on the measurement device geometry is measured to determine the relative resistance to rotation, following ASTM D4402/D4402M-23 [49].
- Dynamic Shear Rheometer (DSR): A Malvern Kinexus Ultra Plus rotational rheometer was used to evaluate the rheological behavior of asphalt binders, following ASTM D7175-23 [50]. The DSR test assesses binder performance at specific temperatures and loading conditions by measuring the phase angle ( $\delta$ ) and complex shear modulus ( $G^*$ ), which indicate binder stiffness and resistance to deformation. Rutting resistance is determined by analyzing  $G^*/\sin \delta$  values. The test was conducted at 88°C.

### 2.2.2. Chemical Properties

The chemical interactions between asphalt cement (AC) and hard resin from Yang (HY) were examined through a range of microstructural and chemical characterization techniques, as follows:

- Environment Scanning Electron Microscopy (ESEM): ESEM was used to analyze the surface characteristics of asphalt samples under controlled environmental conditions. This technique enables high-resolution imaging, providing insights into microstructural features and material interactions.
- Fourier Transform Infrared Spectroscopy (FT-IR): A Bruker Model TENSOR27 spectrometer was used for FT-IR analysis, an analytical technique employed to identify and differentiate organic, polymeric, and select inorganic compounds based on their infrared absorption spectra.
- X-Ray Diffraction (XRD): A PANalytical X'Pert PRO diffractometer was used for XRD analysis, a non-destructive technique that provides detailed insights into precursor molecules, physical properties, and crystallographic structure of the material.
- Differential Scanning Calorimetry (DSC): A METTLER TOLEDO DSC 3 Plus was used for DSC analysis, a thermoanalytical technique that measures the heat flow difference between a sample and a reference as a function of temperature.
- Nuclear Magnetic Resonance (NMR): A Bruker Model Ascend-400 spectrometer was used for NMR analysis, a powerful technique for determining the structural and chemical properties of molecules. Specifically,  $^1\text{H}$  NMR spectroscopy analyzes hydrogen nuclei (protons) in a molecule, using chloroform ( $\text{CDCl}_3$ ) as a solvent, where hydrogen (H) is replaced by deuterium (D).

### 2.2.3. Mechanical Properties

The Marshall method was employed to evaluate the mechanical properties of asphalt concrete in accordance with ASTM D6927-22 [51]. This procedure was used to determine the optimum binder content (OBC), focusing on volumetric properties such as density, air voids, voids filled with bitumen (VFB), and voids in mineral aggregate (VMA). In line with the Thai standard, the OBC was determined within a range of 3% to 7% [52]. Preparation of the asphalt mixtures involved the selection of specific aggregate types and asphalt concrete wearing courses to assess mixture performance. The wearing course, which forms the uppermost pavement layer, is designed to resist traffic loads, limit water infiltration, and improve skid resistance. It typically consists of asphalt concrete with controlled aggregate gradation and binder content to ensure durability, stability, and long-term performance. Sieve analysis was conducted to determine aggregate gradation, as particle size distribution critically influences the strength and density of pavement structures. In this study, the selected gradation satisfied the upper and lower specification limits, confirming its suitability for the mix design, as shown in Figure 5.

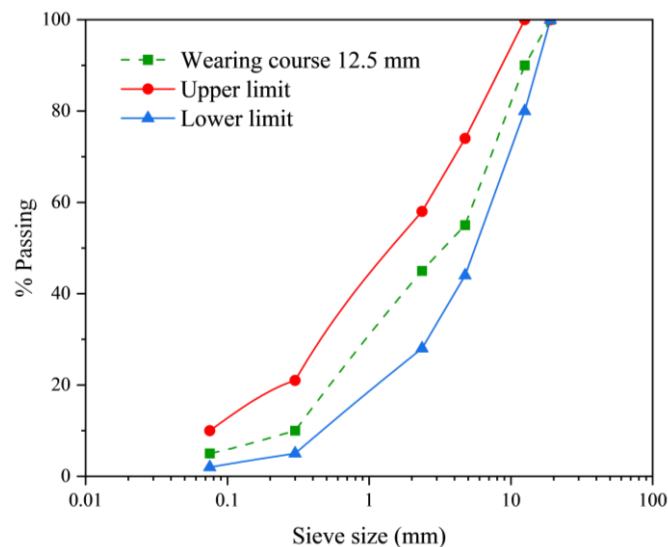


Figure 5. Gradation of aggregate in asphalt concrete mixture

### 3. Results and Discussion

This section examines the effects of hard resin from Yang (HY) on the physical, rheological, thermal, chemical, and mechanical properties of natural rubber–modified asphalt (NRMA). The objective is to identify an optimal HY dosage that enhances binder performance without compromising structural integrity or workability. Results are interpreted with respect to engineering significance, molecular behavior, and practical implications for pavement applications. Particular emphasis is placed on the interaction between HY and the asphalt matrix, as well as on the influence of varying HY contents (3%, 7%, and 15% by weight) on key performance indicators such as stiffness, flexibility, and deformation resistance. Each subsection presents specific test outcomes and compares them with previous studies, thereby underscoring the novelty and relevance of HY as a sustainable bio-based asphalt modifier.

#### 3.1. Penetration Test

The penetration test serves as a fundamental indicator of asphalt binder consistency, reflecting stiffness and susceptibility to deformation under load. Lower penetration values correspond to harder, rut-resistant binders, whereas higher values indicate softer and more flexible materials [46]. As shown in Figure 6, the original asphalt cement (AC) exhibited a penetration of 98 dmm (0.1 mm = 1 dmm), while the hard resin from Yang (HY) showed a substantially higher value of 127 dmm, indicative of lower stiffness and a thermoplastic nature. Under TIS 851-2018 and ASTM D5-13 standards [44, 46], asphalt cements are classified by penetration grade, with AC80–100 representing values between 80 and 100 dmm at 25 °C. This grade is widely applied in moderate to warm climates as it balances stiffness and flexibility. It is softer and more workable than AC60–70, yet provides greater rutting resistance than AC100–120.

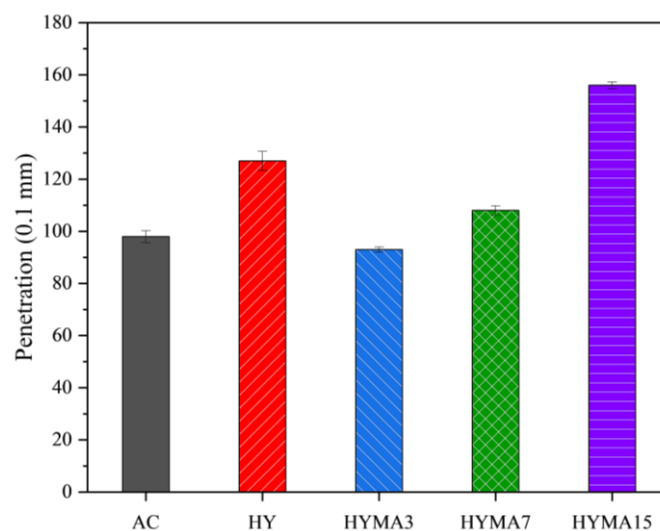


Figure 6. Penetration test results



Incorporation of HY at 3%, 7%, and 15% by weight (HYMA3, HYMA7, and HYMA15) yielded penetration values of 93, 108, and 156 dmm, respectively. HYMA7 and HYMA15 followed the expected plasticizing trend, whereas HYMA3 exhibited a slightly lower value than AC. This deviation may be attributed to experimental variability or complex molecular interactions at low concentrations, warranting further investigation. The progressive increase observed in HYMA7 and HYMA15 confirms the direct relationship between HY dosage and binder softening, consistent with rheological and chemical evidence.

The softening effect at higher HY levels aligns with Jitsangiam et al. [15], who reported that natural rubber-modified asphalt softens at elevated modifier contents due to disruption of matrix integrity. Similar results by Tuntiworawit et al. [53] and Al-Mansob et al. [54] emphasize the importance of dosage optimization when employing bio-based modifiers to balance performance gains against softening effects. Integrating NR with bio-oils from waste resources further mitigates individual limitations while supporting recycling and sustainability.

Complementary ESEM and FTIR analyses supported the penetration test results, as illustrated in Figures 7 and 8, respectively. ESEM images showed improved surface uniformity in HYMA3 and HYMA7, whereas HYMA15 exhibited clustering and reduced homogeneity. The absence of new chemical bonds or cross-linking in FTIR spectra confirmed that the changes were physical rather than chemical [18], reinforcing the plasticizing mechanism of HY.

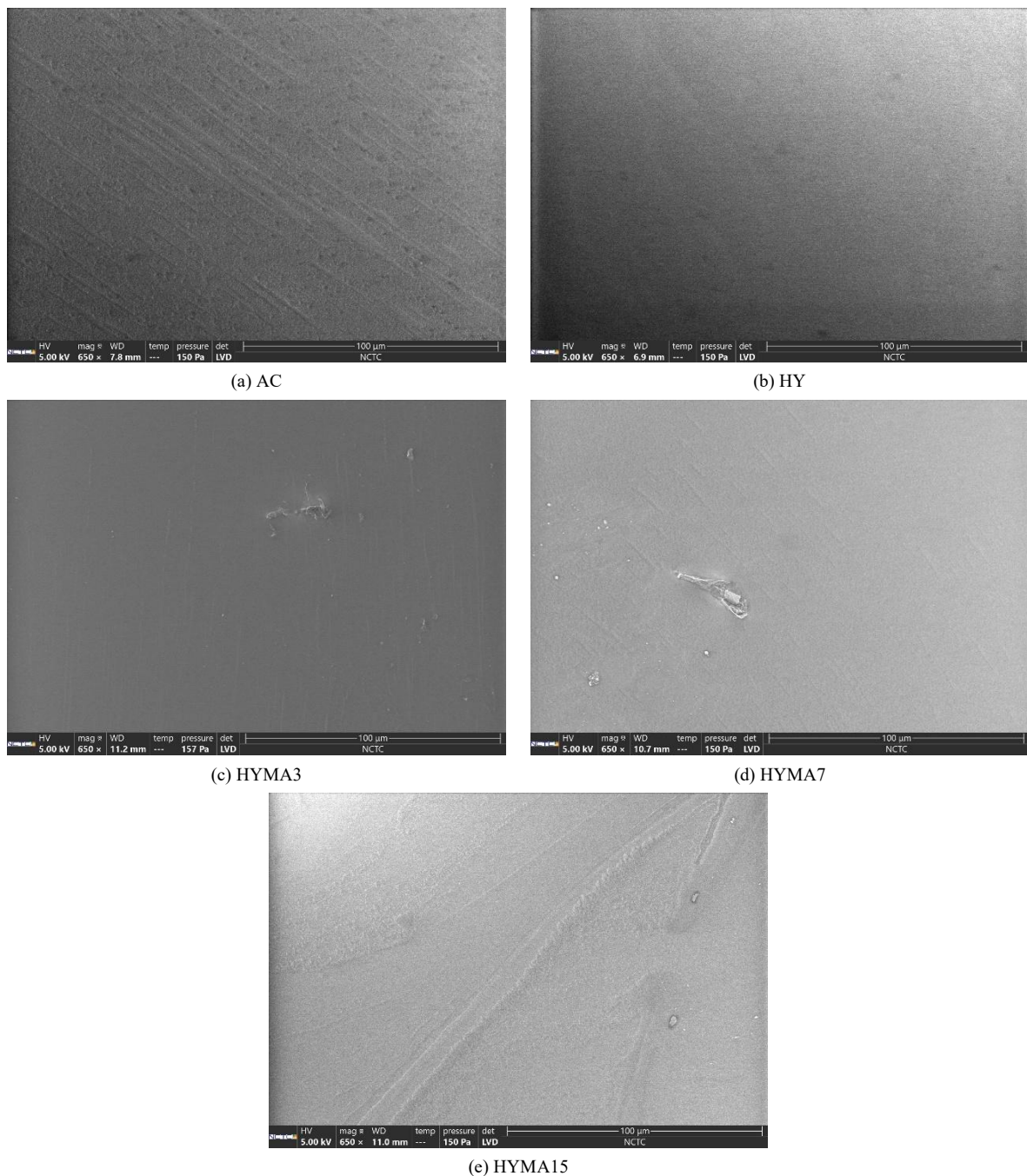
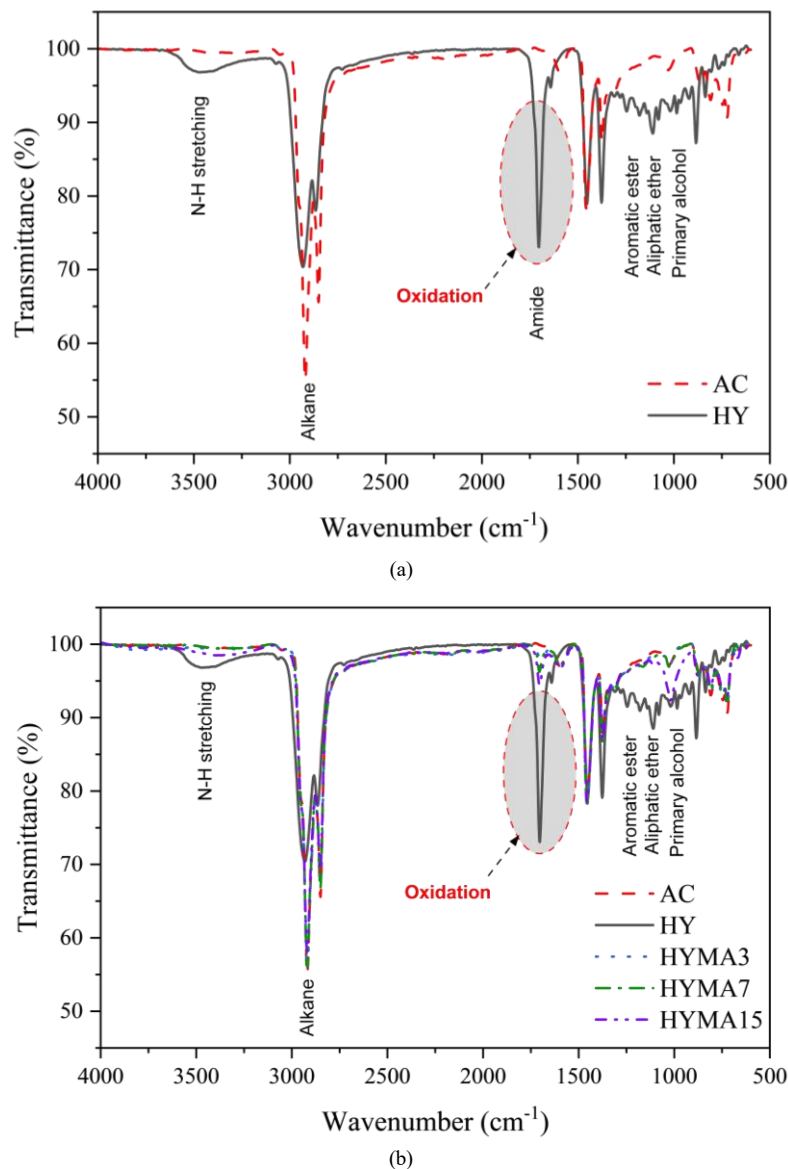


Figure 7. Surface morphology



**Figure 8. Fourier transform infrared spectroscopy (FT-IR) results: (a) Comparison of bands between AC and HY, (b) Comparative analysis of AC and modified asphalt binder with varying HY contents**

In summary, penetration results demonstrate that HY contents  $\geq 7\%$  progressively soften the binder, with optimum performance likely achieved at lower concentrations where the balance between workability and structural integrity is preserved. These findings highlight the promise of HY as a sustainable asphalt additive, provided that dosage is carefully optimized for warm-climate flexible pavement applications.

### 3.2. Ductility Test

The ductility test evaluates the ability of asphalt binders to elongate before rupture, thereby reflecting their flexibility and resistance to thermal cracking. As shown in Figure 9, the original asphalt cement (AC) exhibited a ductility value of 100 cm, indicating high flexibility suitable for hot-climate pavements such as those in Thailand, while also satisfying the minimum requirement of the TIS 851-2018 standard [44]. In contrast, the pure HY binder displayed a markedly lower ductility of 40 cm, reflecting reduced cohesive strength and limited elongation capacity.

Incorporation of HY into NRMA resulted in a progressive decline in ductility with increasing HY content. HYMA3 retained a ductility of 100 cm—equivalent to AC and compliant with TIS 851-2018 [44]—whereas HYMA7 and HYMA15 exhibited reduced values. This trend is consistent with the findings of Tuntiworawit et al. [53] and Jitsangiam et al. [15], who reported similar decreases in elongation with higher modifier dosages. These studies emphasize that while small amounts of additive can preserve flexibility, excessive contents disrupt matrix continuity and reduce extensibility. The diminished elongation capacity of HY is attributed to its weaker intermolecular cohesion compared with the continuous hydrocarbon network of AC.



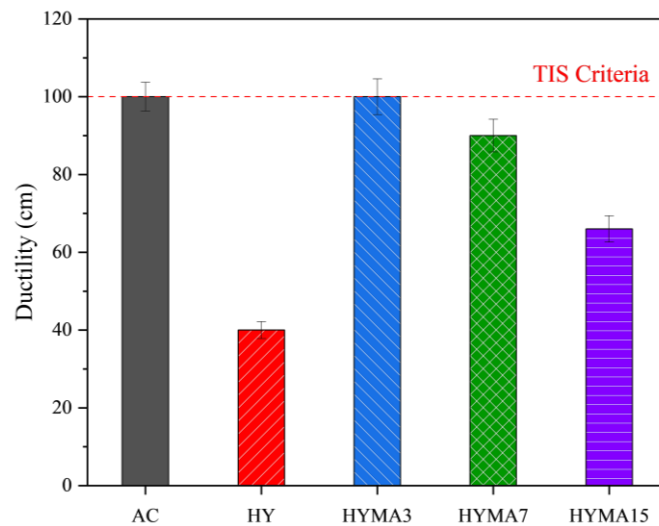


Figure 9. Ductility test results

The observed reduction in ductility with higher HY contents confirms a disruption of molecular cohesion within the asphalt matrix, indicating that HY acts primarily as a softening modifier. Although it decreases stiffness, it simultaneously reduces extensibility—a behavior consistent with the increased penetration values and reduced complex modulus obtained from rheological testing.

Overall, HYMA3 achieved the most favorable balance between flexibility and cohesion, demonstrating its suitability for tropical pavements that require resistance to both cracking and deformation, while maintaining compliance with the TIS 851-2018 [44] standard.

### 3.3. Softening Point Test

The softening point test reflects the temperature sensitivity of asphalt binders and their transition from a semi-solid to a viscous state. In tropical climates, such as Thailand, where pavement surface temperatures typically range from 45 °C to 60 °C during peak hours, maintaining a high softening point is crucial to minimize permanent deformation under thermal loading and to enhance long-term rutting resistance.

As shown in Figure 10, the original asphalt cement (AC) exhibited a softening point of 47 °C, which falls within the TIS 851-2018 [44] standard range of 42 to 52 °C for AC80-100. In contrast, HY displayed a significantly lower value of 41 °C, indicating inferior thermal resistance compared with AC. Incorporation of HY into asphalt binders produced dosage-dependent responses. HYMA3 exhibited a softening point of 46.7 °C, which is closely comparable to AC and fully compliant with TIS 851-2018 [44], making it the most thermally stable among the modified binders. The negligible reduction at 3% HY suggests that the AC matrix still dominates the thermal behavior, while the influence of HY, characterized by carbonyl functional groups (C=O) and shorter hydrocarbon chains with lower thermal stability, becomes more pronounced at higher concentrations.

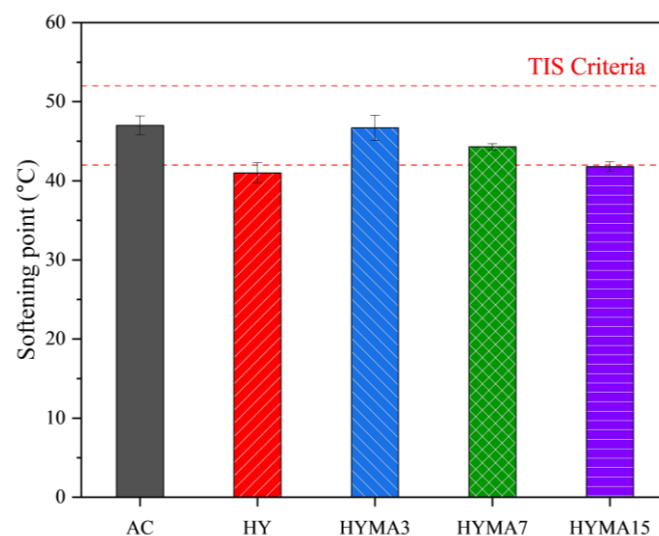


Figure 10. Softening point results

Increasing HY contents in HYMA7 and HYMA15 progressively reduced the softening points to 44.3 °C and 41.8 °C, respectively, reflecting the growing influence of HY on the thermal response. Although both values remain within TIS 851-2018 [44] limits, HYMA15 approaches the lower threshold. These findings are consistent with Zahoor et al. [19], who reported that higher proportions of soft, low-molecular-weight bio-oils reduce the softening point of asphalt blends depending on mixture composition. In this study, the reduction corresponds to the transition from AC-dominated to HY-dominated thermal behavior, as further supported by FTIR results indicating physical blending without chemical modification.

In summary, HYMA3 emerged as the most suitable formulation for warm-climate applications, combining thermal stability comparable to AC with enhanced workability from HY incorporation while maintaining compliance with TIS 851-2018 [44]. In contrast, HYMA7 at 44.3 °C and HYMA15 at 41.8 °C, though still within standard limits, approach critical thresholds for tropical service conditions and may therefore be better suited for moderate traffic pavements, secondary layers, or regions with less severe thermal exposure where improved workability outweighs reduced thermal stability.

### 3.4. Viscosity Test

The viscosity test evaluated the resistance of asphalt binders to flow at elevated temperatures and provided critical insight into their suitability for mixing, pumping, and compaction, following ASTM D4402/D4402M-23 [49]. As shown in Figure 3, viscosity was measured over the temperature range of 45 °C to 120 °C, where 45 °C represented the lower bound above the softening points of both materials, and 120 °C reflected the typical mixing temperature in asphalt production.

At lower temperatures between 45°C and 55°C, HY exhibited higher viscosity than AC, which appeared inconsistent with its lower softening point and higher penetration values. This apparent inconsistency arose from different molecular mechanisms governing viscosity compared with those governing penetration or softening point. The elevated viscosity of HY at low temperatures likely resulted from its resinous molecular structure containing aromatic compounds and polar groups, which generated stronger intermolecular interactions and increased resistance to flow despite the softer consistency indicated by other tests. At approximately 60 °C, the viscosity of AC surpassed that of HY and the HY-modified binders, indicating a viscosity crossover that reflected differences in thermal sensitivity. This crossover occurred because the resinous components of HY were more thermally sensitive, and their intermolecular interactions degraded more rapidly with temperature than the saturated hydrocarbon structures in AC. Similar temperature-dependent responses were reported in previous studies on bio-modified asphalts, where different test methods highlighted distinct aspects of binder behavior [27, 30].

Among the modified formulations, HYMA15 exhibited the lowest viscosity across all test temperatures, consistent with its high penetration value and reduced softening point. This indicated enhanced flow characteristics that facilitated mixing and laying but might compromise performance under high-temperature service conditions. In contrast, HYMA3 displayed viscosity behavior closely aligned with AC while offering slightly improved flowability, suggesting a favorable balance between thermal workability and structural integrity.

The overall reduction in viscosity with increasing temperature reflects the viscoelastic nature of asphalt binders. Of the tested formulations, HYMA3 exhibited the most favorable balance between workability and performance, underscoring its suitability for hot-mix asphalt applications that require both ease of processing and long-term durability.

### 3.5. Dynamic Shear Rheometer (DSR) Test

The Dynamic Shear Rheometer (DSR) test, conducted in accordance with ASTM D7175-23 [50], is widely used to evaluate the viscoelastic properties of asphalt binders by measuring the complex shear modulus ( $G^*$ ) and phase angle ( $\delta$ ). Figure 11 presents the rutting resistance factor ( $G^*/\sin \delta$ ), a key indicator of high-temperature performance [27]. Among the tested materials, asphalt cement (AC) consistently exhibited the highest  $G^*/\sin \delta$  values, reflecting superior resistance to permanent deformation. HYMA3 and HYMA7 produced values close to AC, indicating that low concentrations of HY can retain satisfactory rheological properties while improving workability. In contrast, HY and HYMA15 displayed markedly lower values, consistent with their higher penetration and lower viscosity observed in Figures 6 and 3, respectively. This reduction highlights the strong plasticizing effect of HY at higher concentrations, which enhances flexibility but reduces rutting resistance.

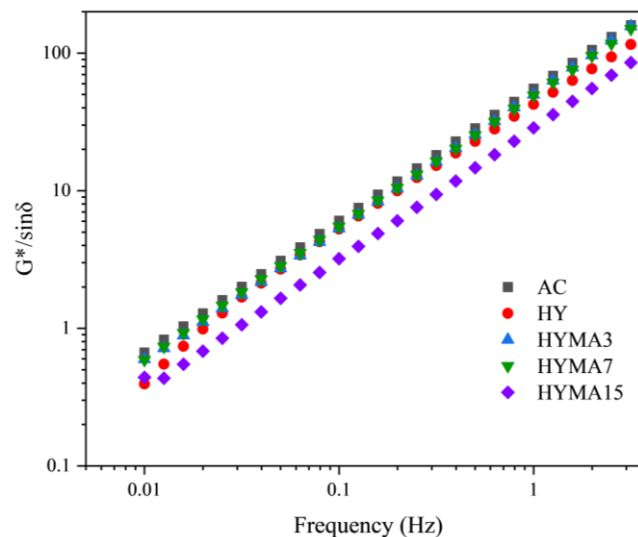


Figure 11. Rutting resistance results

Although HYMA3 and HYMA7 maintained stiffness levels comparable to AC, the performance of HYMA15 decreased sharply, suggesting a critical content range of 7–15% HY beyond which additional modifier impairs high-temperature performance. The rheological behavior of HYMA3 and HYMA7 closely followed that of AC across most frequencies, whereas HY exhibited lower values at both low and high frequencies, converging with AC only at intermediate frequencies. This frequency-dependent response has practical implications for field applications because it corresponds to specific traffic loading and temperature conditions.

To support these rheological findings, microstructural evidence was further examined using ESEM analysis. As illustrated in Figure 7, HYMA3 and HYMA7 retained surface morphologies comparable to AC, characterized by irregular patterns that may have contributed to their preserved rheological performance. This microstructural similarity corroborates the rheological results, suggesting that optimal HY concentrations do not significantly disrupt the asphalt matrix. Collectively, these findings indicate that HYMA3 achieves the most desirable compromise between workability and high-temperature resistance among the tested formulations.

Both AC and HYMA binders exhibited viscoelastic responses, with controlled HY modification (HYMA3, HYMA7) maintaining performance comparable to AC while preserving the viscoelastic balance required for high-temperature conditions. The modification-induced rheological changes align with established principles of bio-modifier–asphalt interactions. These outcomes further support and are consistent with previous findings by Zhang et al. [27] and Ingrassia et al. [22], confirming that controlled bio-modifier incorporation can sustain high-temperature and frequency performance when used at optimal concentrations. Consequently, the bio-binders developed in this study are expected to achieve durability and long-term performance comparable to conventional bitumen, reinforcing their potential as sustainable alternatives to traditional binders.

FTIR spectra revealed no evidence of new functional groups or chemical cross-linking in HYMA formulations, indicating that HY interacts physically rather than chemically with the asphalt matrix, as presented in Figure 8. This confirms that the modification effect is primarily governed by dispersion and phase compatibility rather than molecular bonding. To support the overall conclusion, these spectroscopic results further demonstrate that HY functions as a physical modifier, consistent with the rheological and microstructural findings.

In summary, the DSR results show that HYMA3 provides the most favorable compromise between workability and high-temperature resistance. However, further investigation is required to evaluate long-term durability, aging resistance, and performance under real-world traffic and environmental conditions.

### 3.6. Environment Scanning Electron Microscopy (ESEM)

Environmental Scanning Electron Microscopy (ESEM) was employed to investigate the microstructural features of HY-modified asphalt binders (HYMA). This high-resolution technique provides valuable insight into surface morphology and supports the interpretation of the physical interactions between bitumen and modifying agents [18].

As shown in Figure 7, the surface of the asphalt cement (AC) binder exhibited irregular textures resembling sketch marks, which is consistent with observations reported by Ansari et al. [18]. In contrast, HYMA3 and HYMA7 displayed smoother, layered surface morphologies with preferential orientation, indicating improved dispersion of HY and

enhanced microstructural uniformity. These organized layered patterns further support the rheological observations by suggesting better compatibility between HY and the asphalt matrix at lower concentrations.

At higher concentrations, HYMA15 exhibited a denser and more irregular surface with evident HY clustering, indicative of localized accumulation caused by phase separation. This reduced surface uniformity corresponds to lower stiffness and higher penetration values, thereby supporting the increased penetration and reduced rutting resistance factors observed in the physical and rheological tests. The distinct interfaces observed in HYMA3 and HYMA7 indicate partial miscibility, where physical blending predominates over chemical bonding.

Although ESEM provides useful visual confirmation of modifier dispersion at the surface level, it does not offer conclusive evidence of chemical composition or long-term stability within the bulk material. Therefore, the interpretation of microstructural images should be complemented by chemical and mechanical analyses to support the identification of the most effective HY content and ensure the long-term performance of asphalt binders.

### 3.7. Fourier Transform Infrared Spectroscopy (FT-IR)

Fourier Transform Infrared Spectroscopy (FT-IR) was employed to characterize the chemical bonds and functional groups of asphalt cement (AC), hard resin from Yang (HY), and their blends. The spectra are presented in Figure 8 as percent transmittance versus wavenumber ( $\text{cm}^{-1}$ ).

As shown in Figure 8-a, both AC and HY exhibit major absorption peaks associated with C–H alkane stretching at  $2920.10$  and  $2850.99$   $\text{cm}^{-1}$  (AC), and  $2932.11$  and  $2865.69$   $\text{cm}^{-1}$  (HY). Methyl C–H stretching is observed at  $1457.25$  and  $1374.95$   $\text{cm}^{-1}$  (AC), and  $1452.95$  and  $1376.85$   $\text{cm}^{-1}$  (HY). HY demonstrates additional peaks absent in AC, including N–H stretching at  $3456.86$   $\text{cm}^{-1}$ , C–O stretching signals of aromatic esters in the  $1280$ – $1310$   $\text{cm}^{-1}$  range, aliphatic ethers at  $1110.06$   $\text{cm}^{-1}$ , and primary alcohols at  $1080.37$   $\text{cm}^{-1}$ . A carbonyl (C=O) stretching band at  $1703.92$   $\text{cm}^{-1}$  indicates oxidative degradation products typically found in oxidized natural rubber latex [43]. The AC spectrum contains typical hydrocarbon-related bands, such as aromatic C=C stretching near  $1598.69$   $\text{cm}^{-1}$  and sulfoxide at  $1029.23$   $\text{cm}^{-1}$ . These results align with earlier studies [15, 18, 19], which emphasized the diagnostic value of C–H and C=O signals in evaluating binder modification. Similarly, Zargar et al. [20] identified comparable peaks in rejuvenated asphalt with waste oils, thus confirming the hydrocarbon-dominated nature of bituminous binders.

Figure 8-b shows that the spectra of HY-modified binders gradually resemble that of pure HY with increasing HY content. However, in the fingerprint region ( $1300$ – $500$   $\text{cm}^{-1}$ ), AC-related bands remain prominent, indicating asphalt as the dominant phase within the blends. Importantly, no new absorption bands or chemical shifts were detected, confirming the absence of chemical reactions or cross-linking between HY and AC. This outcome is consistent with the findings of Hazoor Ansari et al. [18], who reported that blending in such systems is primarily governed by physical interactions rather than chemical modification. The overall blend properties therefore arise from a balance between the plasticizing effect of HY and the structural integrity provided by AC. At low HY contents (e.g., HYMA3 and HYMA7), this balance results in effective dispersion, improved workability, and preserved mechanical stiffness. At higher concentrations (e.g., HYMA15), phase separation and localized clustering become more evident, leading to reduced uniformity and inconsistent performance.

In summary, FT-IR analysis confirms that HY incorporation does not induce chemical transformation within the asphalt matrix. Instead, property variations observed in mechanical and rheological tests are attributed to physical interactions. This interpretation is reinforced by ESEM results, which revealed uniform morphologies at low HY levels and clustering at high contents, as well as by DSR testing, which demonstrated that HYMA3 and HYMA7 maintained high-temperature stiffness comparable to AC, whereas HYMA15 exhibited a marked decline. Collectively, these findings highlight that optimal HY incorporation relies on achieving uniform physical interaction, with low dosages providing the most effective balance between enhanced workability and sustained high-temperature resistance.

### 3.8. X-Ray Diffraction (XRD)

X-ray diffraction (XRD) analysis was performed to investigate the crystalline and amorphous phases of asphalt cement (AC), hard resin from Yang (HY), and HY-modified asphalt binders (HYMA). This technique provides insight into structural ordering by examining diffraction peak positions and intensities, thereby allowing the evaluation of molecular arrangement and the degree of ordering [55].

As illustrated in Figure 12, both AC and HYMA3 exhibited two main peaks at approximately  $14^\circ$  and  $16.8^\circ$ , representing the coexistence of ordered and disordered molecular domains commonly associated with semicrystalline polymer systems. These diffraction patterns are consistent with earlier findings reported for asphalt cement by Siddiqui et al. [55] and for natural rubber latex (NRL)-modified asphalt by Jitsangiam et al. [15]. A minor peak observed near  $20^\circ$  further suggests localized molecular ordering within these samples.

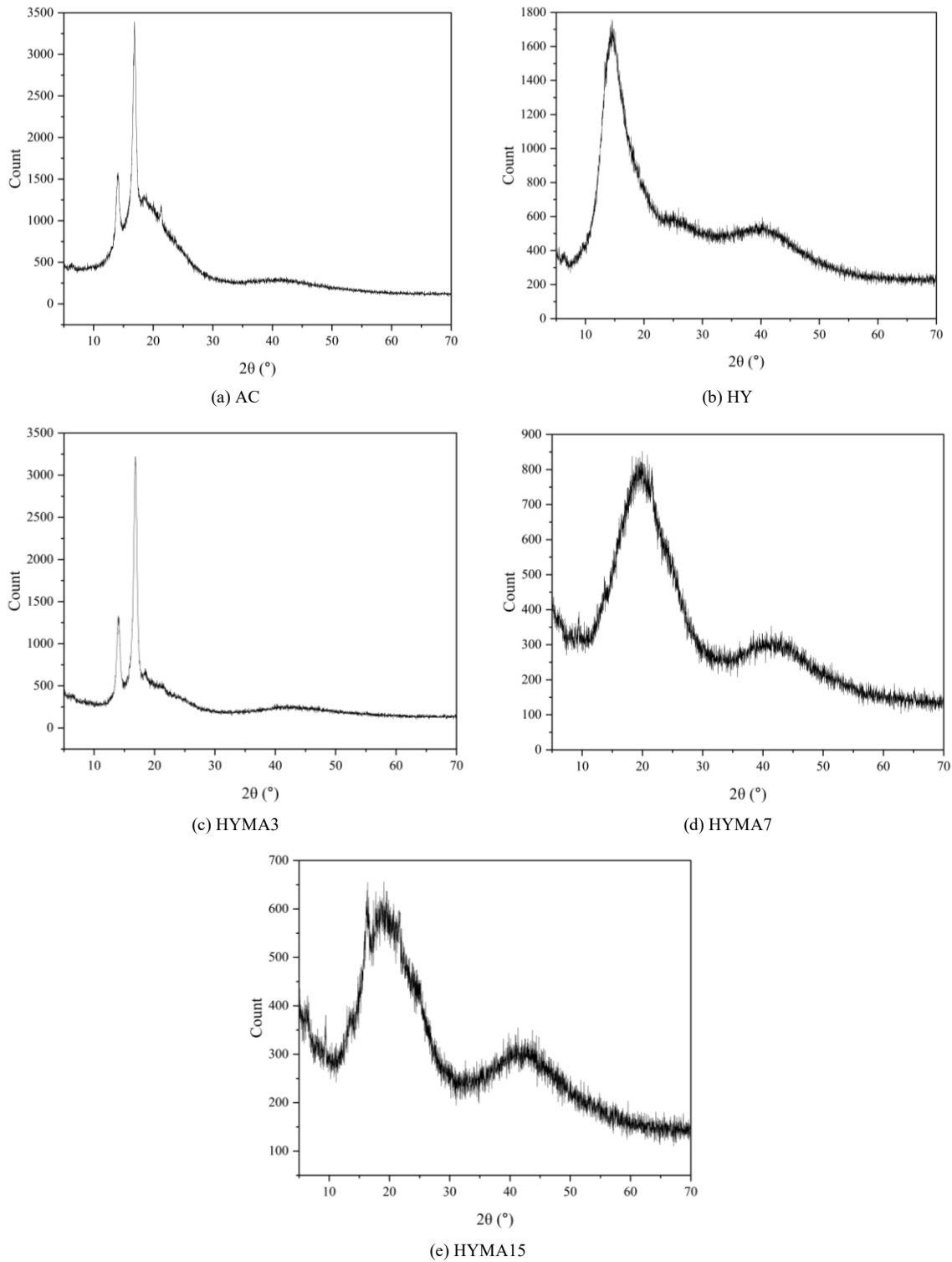


**Figure 12. XRD analysis result**

In contrast, HY displayed its most pronounced peak at  $14^\circ$ , corresponding to the position observed in AC but with considerably lower intensity, reflecting a predominantly amorphous structure characteristic of irregular molecular arrangements in natural polymer extracts. As the HY content increased in HYMA7 and HYMA15, the diffraction peaks became progressively weaker and less distinct, indicating reduced molecular ordering and the growing dominance of amorphous domains.

The diminished sharpness and intensity of peaks in HYMA7 and HYMA15 confirm their predominantly amorphous character, which corresponds with the higher penetration values and reduced stiffness observed in mechanical testing. This structural modification can be attributed to the disruption of regular molecular packing by HY molecules, which interferes with ordered domains and weakens intermolecular correlations.



In summary, XRD results demonstrate that increasing HY concentration in asphalt binders promotes a transition toward amorphous morphology. This structural shift directly affects molecular organization and correlates with reduced stiffness and mechanical performance, reinforcing the interpretation that HY interacts physically with AC rather than chemically. These findings complement the FT-IR results, which showed no chemical bonding, and the ESEM observations, which revealed phase separation at high HY levels.

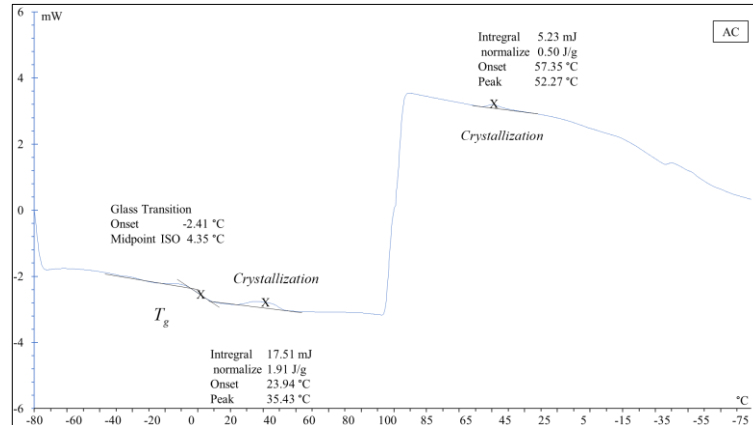
### 3.9. Differential Scanning Calorimetry (DSC)

Differential Scanning Calorimetry (DSC) was employed to investigate thermal transitions and phase behavior in asphalt cement (AC), hard resin from Yang (HY), and HY-modified blends. This technique provides essential information—including the glass transition temperature ( $T_g$ ), crystallization behavior, and other thermal events—that influence asphalt performance over a wide range of service temperatures. The  $T_g$  is particularly significant, as it represents the transition of a material from a rigid, glassy state to a flexible, viscoelastic condition [31].

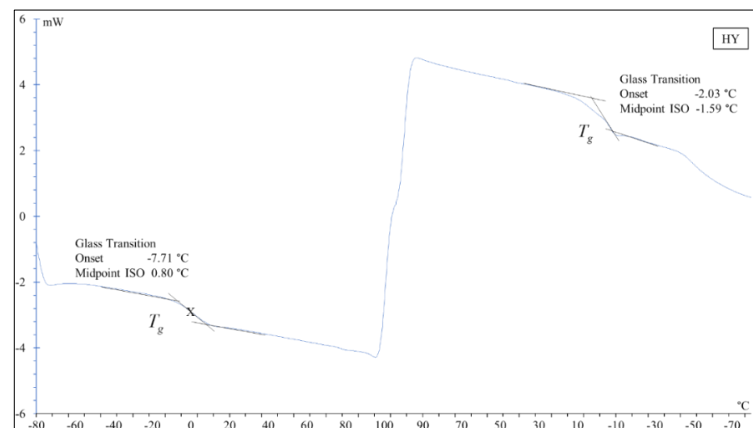
As summarized in Table 3 and shown in Figure 13, neat AC exhibited a  $T_g$  of 4.35 °C and a crystallization peak at 35.43 °C during heating. During cooling, AC crystallized at 52.27 °C, whereas no distinct  $T_g$  was detected, likely due to overlapping transitions within its complex molecular structure. By contrast, HY showed markedly lower  $T_g$  values of 0.80 °C (heating) and −1.59 °C (cooling), with no distinct crystallization peaks, indicating a predominantly amorphous morphology and confirming its intrinsic plasticizing effect.

**Table 3. DSC analysis result**

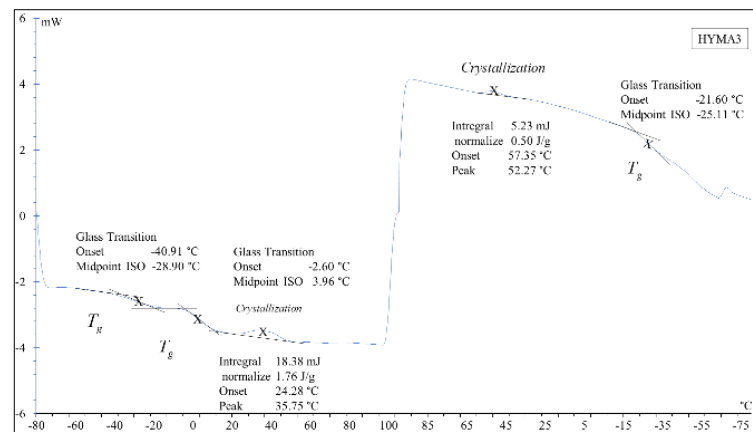
Temp. zone	-80 °C to 100 °C			100 °C to -80 °C	
Type	$T_g$ (°C)	$T_g$ (°C)	Crystallization (°C)	Crystallization (°C)	$T_g$ (°C)
AC	4.35	-	35.43	52.27	-
HY	0.80	-	-	-	-1.59
HYMA3	-28.90	3.96	35.75	52.27	-25.11
HYMA7	-28.87	1.20	35.57	51.61	-
HYMA15	-33.98	2.61	35.58	51.10	-



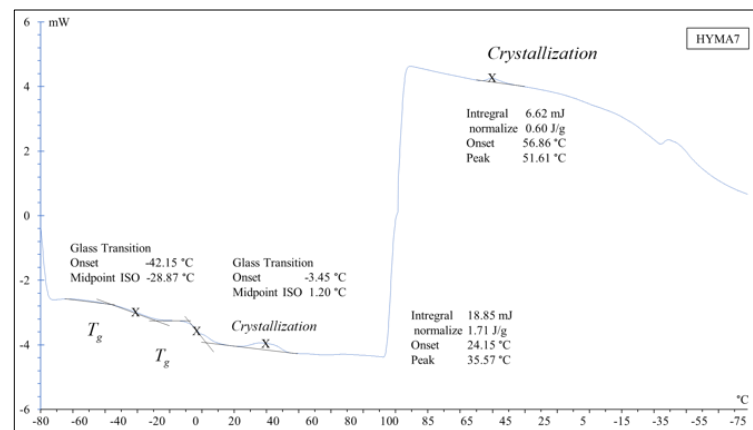
(a) AC



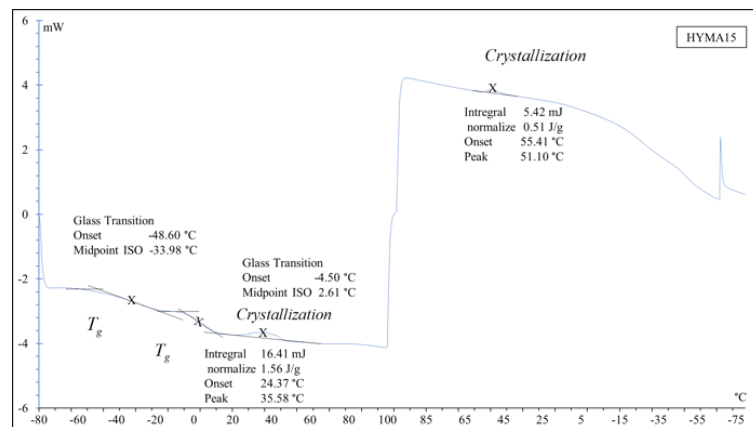
(b) HY



(c) HYMA3



(d) HYMA7



(e) HYMA15

**Figure 13. DSC results**

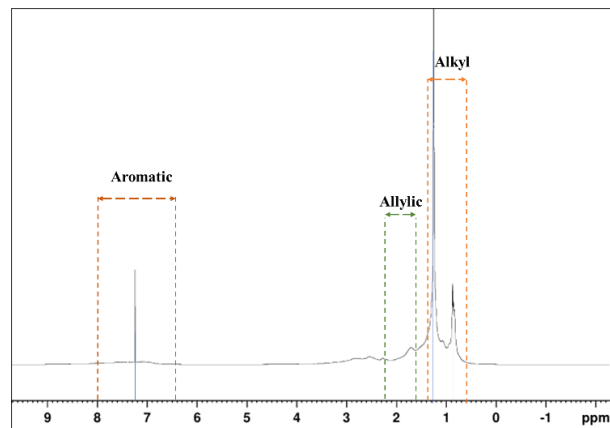
HY-modified asphalt binders (HYMA) exhibited two distinct  $T_g$  values during heating, along with the higher  $T_g$  associated with the asphalt phase. The presence of multiple glass transitions indicates that the blends form a heterogeneous, multiphase system, which likely results from partial miscibility or phase separation between HY and asphalt components. The crystallization temperatures of all HYMA blends remained close to those of neat AC ( $\approx 35^\circ\text{C}$  during heating and  $\approx 51^\circ\text{C}$  during cooling), confirming that crystalline behavior is still governed by the asphalt matrix.

The reduction in  $T_g$  across HYMA blends—particularly in HYMA15—demonstrates enhanced low-temperature flexibility, which is advantageous for mitigating thermal cracking in cold climates. Among the blends, HYMA3 achieved the most favorable balance, improving low-temperature ductility while maintaining structural integrity, consistent with previous reports on optimal modifier dosages [31]. Importantly, all observed transitions occurred within the operational temperature range of flexible pavements, supporting the suitability of HY-modified binders under diverse climatic conditions.

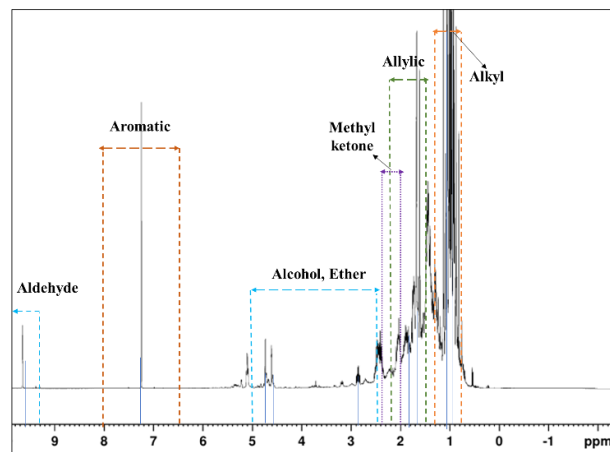
Overall, DSC analysis confirms that the incorporation of HY introduces additional thermal transition phases while preserving the key crystallization characteristics of asphalt. This modification enhances low-temperature performance without compromising thermal stability, reinforcing the potential of HY-based NRMA as a sustainable and climate-resilient binder for pavement applications. Moreover, the multiphase behavior identified in DSC is consistent with the diminished ordering observed in XRD analysis and the physical interactions indicated by FT-IR spectra, collectively supporting the interpretation that HY disrupts molecular packing within the asphalt matrix and promotes amorphous morphology.

### 3.10. Nuclear Magnetic Resonance (NMR)

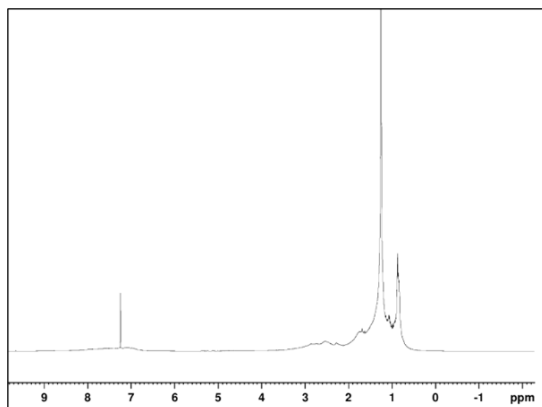
Nuclear Magnetic Resonance (NMR) spectroscopy was employed to investigate the molecular structures and hydrogen environments of asphalt cement (AC), hard resin from Yang (HY), and HY-modified asphalt (HYMA) blends. Deuterated chloroform ( $\text{CDCl}_3$ ) served as the solvent for  $^1\text{H}$  NMR analysis [56]. The spectra in Figure 14 illustrates chemical shift distributions that reflect distinct hydrogen arrangements and possible molecular interactions.



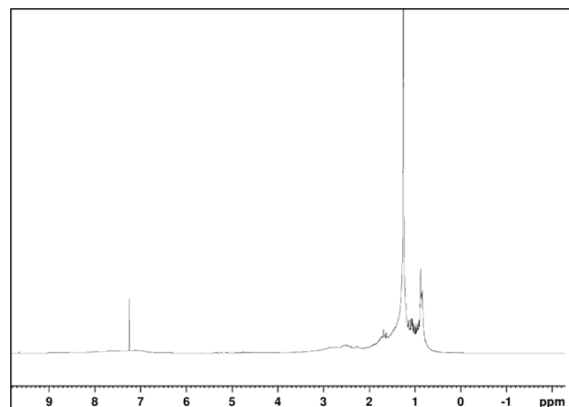
(a) AC



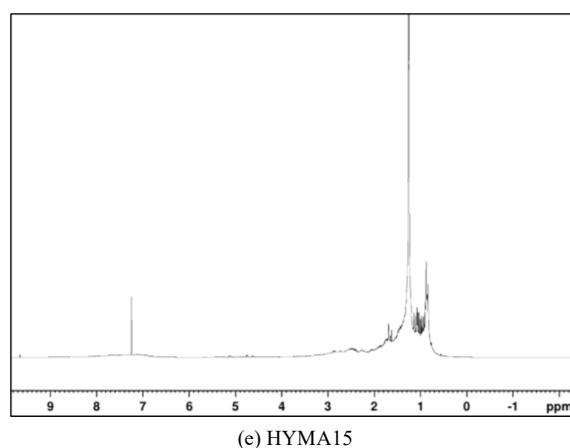
(b) HY



(c) HYMA3



(d) HYMA7



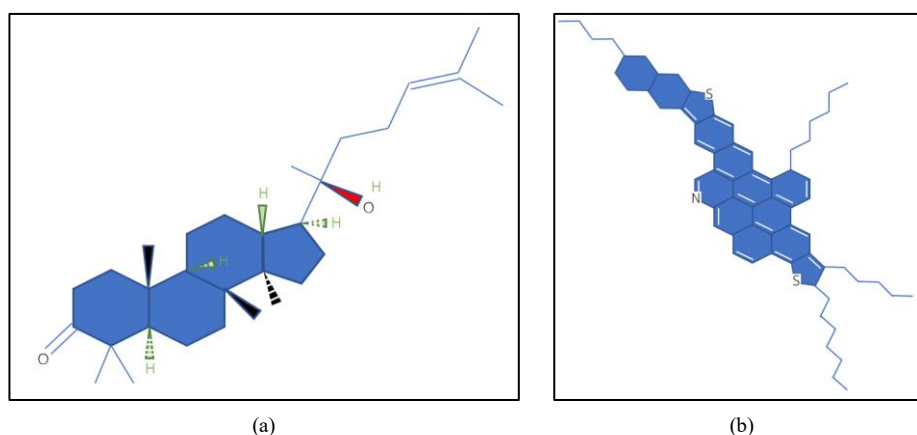
**Figure 14.  $^1\text{H}$  NMR spectra results**

Figure 14-a presents the AC spectrum, which displays characteristic signals for aromatic protons (Ar-H, 6.5–8.0 ppm), allylic protons ( $\text{R}-\text{C}=\text{C}-\text{CH}_3$ , 1.6–2.2 ppm), and alkyl chain protons ( $-\text{CH}_3$ , 0.7–1.3 ppm), confirming the aromatic-rich hydrocarbon framework of AC. In contrast, Figure 14-b shows that HY contains additional signals absent in AC, including peaks corresponding to methyl ketones ( $\text{R}-\text{CO}-\text{CH}_3$ , 2.0–2.4 ppm), alcohols and ethers (2.5–5.0 ppm), and aldehydes (9.0–10.0 ppm). These oxygenated functionalities are consistent with the diterpene alcohol structure of dipterocarpol, the major component of HY, as illustrated in Figure 15-a, and corroborate FTIR evidence of O-H and C=O groups, highlighting oxidation-related chemistry.

The spectra of HYMA3, HYMA7, and HYMA15, illustrated in Figures 14-c to 14-e, reveal a progressive reduction in aromatic intensity and an increase in aliphatic, aldehyde, and other oxygenated signals with rising HY content. Peaks observed at 5.1–5.4 ppm correspond to alkene ( $\text{C}=\text{C}$ ) protons, while signals in the 0.8–1.5 ppm region represent general alkyl ( $\text{R}-\text{CH}_3$ ) hydrogens common to both AC and HY. These spectral variations suggest molecular-level interactions and physical blending between HY and the asphalt matrix, and they align with the concentration-dependent performance trends observed in mechanical testing.

Comparative analysis with FTIR further confirms that alcohol, ether, and carbonyl groups originate from HY incorporation rather than AC. The complementary evidence from both techniques demonstrates that HY–asphalt interactions are primarily physical, as no new chemical environments or significant chemical shift changes were detected that would indicate covalent bonding or cross-linking. This interpretation is consistent with the literature, which highlights the contrast between the hydrocarbon framework of asphalt and the oxygenated terpenoid structure characteristic of Yang resin [15, 43].

Figure 15 illustrates the representative chemical structures of HY and asphalt cement. The structural differences between dipterocarpol, as illustrated in Figure 15-a, and asphaltene, as depicted in Figure 15-b, explain the observed interaction mechanisms in HY-modified binders. The presence of polar functional groups in dipterocarpol enables non-covalent interactions with asphalt components, producing the plasticizing effects observed in rheological testing, including lower softening point, increased penetration, and enhanced flexibility. These structural characteristics strongly support the physical blending mechanism identified across multiple analytical techniques, rather than chemical cross-linking.



**Figure 15. Chemical structures of (a) Dipterocarpol (adapted from Puthongking et al. [43]) and (b) Asphaltene (adapted from Jitsangiam et al. [15])**

In summary, NMR spectroscopy provides strong evidence that HY incorporation modifies asphalt through physical blending rather than chemical transformation, with spectral changes reflecting compositional variation rather than new chemical environments. Combined with FTIR results, these findings conclusively demonstrate that HY functions as a physical modifier through intermolecular interactions rather than covalent bonding. This mechanistic understanding contributes to performance optimization in asphalt formulations and supports the development of more flexible and workable binders for pavement applications.

### 3.11. Mechanical Properties of Asphalt Concrete

The mechanical performance of asphalt concrete was evaluated using Marshall stability and flow tests, as illustrated in Figure 16 [48]. Figure 16-a shows that stability values followed a bell-shaped trend, with the peak corresponding to the optimum binder content (OBC). Conventional asphalt cement (AC) achieved the highest stability of 26.94 kN at an OBC of approximately 5%. In comparison, the stability values for HY, HYMA3, HYMA7, and HYMA15 were 19.65 kN, 23.01 kN, 20.51 kN, and 16.05 kN, respectively. All mixtures exceeded the minimum requirement of 8 kN specified in the Thai standards [52]. Among the HY-modified binders, HYMA3 attained the highest stability, reflecting an optimal balance between matrix cohesion and modifier interaction. Conversely, HYMA15 exhibited the lowest stability due to excessive HY content, which disrupted intermolecular packing and weakened load transfer within the aggregate–binder system. This decline in performance is consistent with viscosity and rutting resistance trends, as shown in Figures 3 and 11, confirming that over-modification reduces structural integrity and compromises long-term durability under traffic loading.

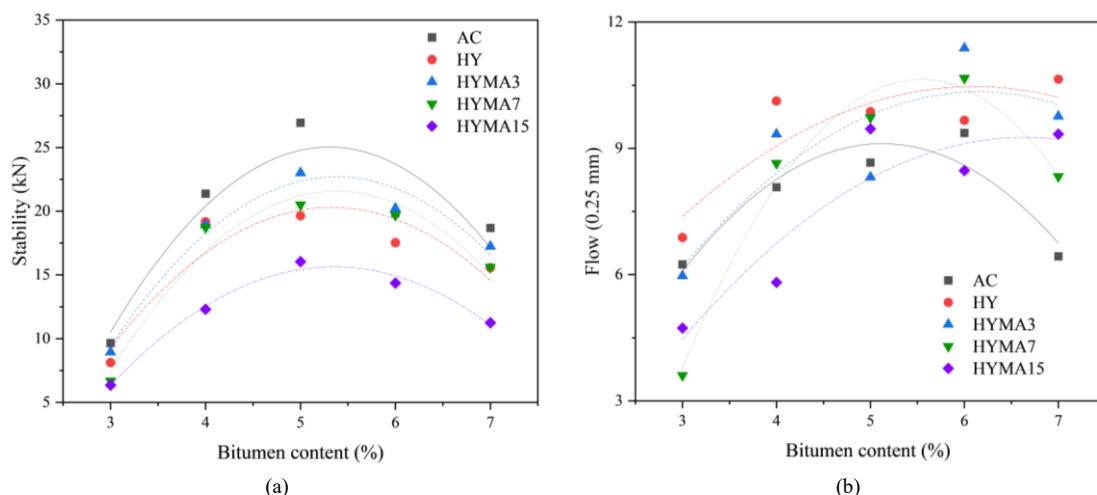


Figure 16. Mechanical properties of asphalt concrete: (a) Stability versus bitumen content and (b) Flow versus bitumen content

Figure 16-b presents the Marshall flow results. AC, HY, and HYMA3 exhibited comparable flow characteristics, whereas HYMA7 and HYMA15 displayed significantly higher flow values, indicating increased binder plasticity. Flow generally increased with binder content, reaching a maximum at approximately 7%, beyond which excess binder reduced aggregate interlock and load-bearing capacity. Nevertheless, all flow values remained within the specification range of 8–16 units (0.25 mm), confirming their suitability for flexible pavement applications [52].

The volumetric properties are summarized in Figure 17. Air voids decreased with increasing binder content, indicating improved binder distribution and compaction. AC mixtures achieved the highest density, while HYMA blends showed greater variability, likely due to differences in HY viscosity and molecular structure. Voids in mineral aggregate (VMA) were relatively stable in AC and HY mixtures but followed a reversed bell-shaped curve in HYMA blends, which is characteristic of modified systems [51]. Voids filled with bitumen (VFB) increased with binder content, reflecting enhanced aggregate coating and reduced total voids.

Overall, HYMA-modified mixtures demonstrated satisfactory mechanical and volumetric performance for pavement applications. However, higher HY dosages impaired compaction efficiency and stability, resulting in less effective air void control. Among the tested blends, HYMA3 offered the most favorable compromise between strength, flexibility, and workability. These results provide quantitative guidelines for the incorporation of HY in asphalt mixtures, ensuring structural reliability while supporting sustainable pavement design.



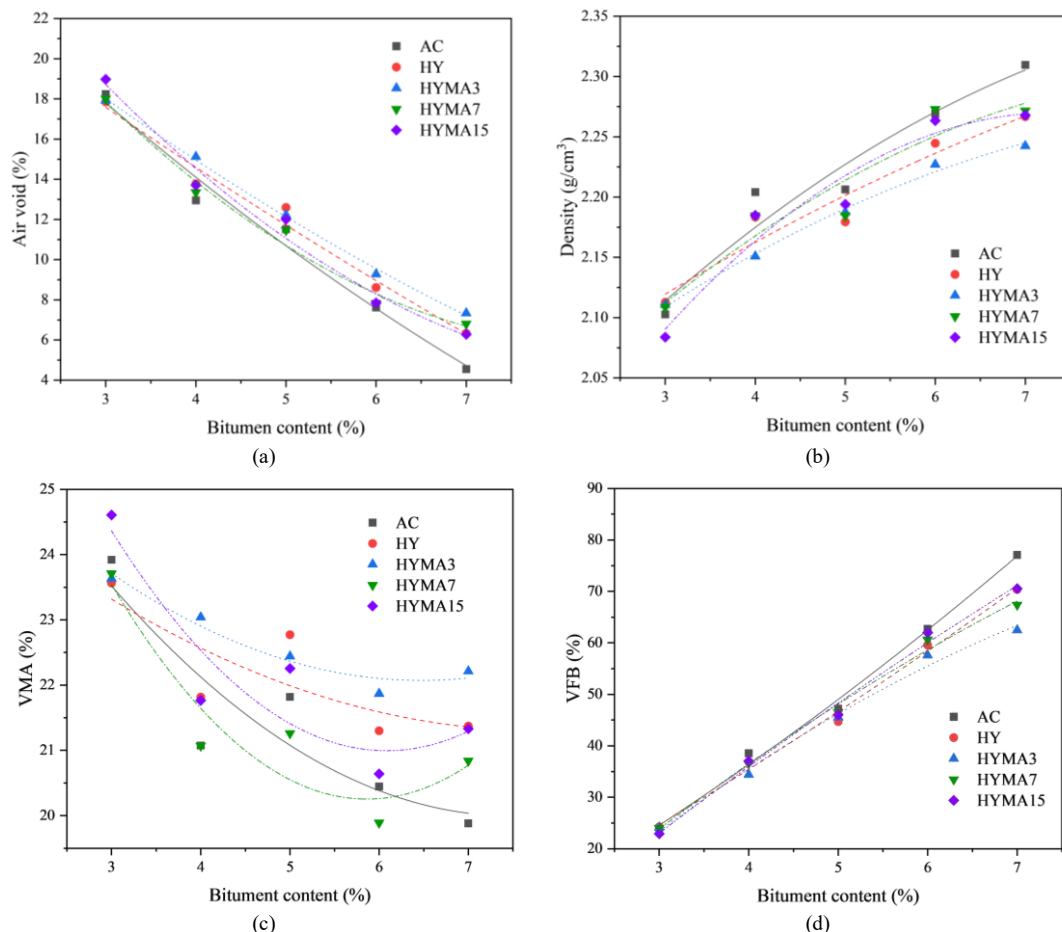


Figure 17. Volumetric properties of asphalt concrete: (a) Air voids versus bitumen content, (b) Density versus bitumen content, (c) VMA versus bitumen content, and (d) VFB versus bitumen content

## 4. Conclusion

This study investigated the influence of hard resin derived from Yang (HY), a renewable bio-based byproduct, on the performance of natural rubber-modified asphalt (NRMA). The findings revealed that HY substantially alters binder viscoelasticity by affecting penetration, viscosity, and rutting resistance. Among the tested formulations, HYMA3 (3% HY) provided the most favorable balance between stiffness and flexibility, identifying it as the optimal dosage for flexible pavement applications. In contrast, higher HY dosages ( $\geq 7\%$ ) resulted in excessive softening and diminished cohesion, thereby compromising performance.

Chemical analyses (FT-IR and NMR) confirmed the presence of oxygenated functional groups in HY but showed no evidence of chemical cross-linking, indicating that modification primarily occurs through physical blending. Complementary structural and thermal evaluations using XRD, ESEM, and DSC demonstrated reduced crystallinity, morphological reorganization, and enhanced low-temperature flexibility. Mechanical and volumetric assessments further validated that HYMA3 exhibited superior compaction and stable air-void distribution, reinforcing its practical applicability.

Overall, the incorporation of HY enhances binder performance while simultaneously promoting sustainability by transforming an underutilized natural byproduct into a functional construction additive. This research provides the first comprehensive characterization of Yang resin as an asphalt modifier, establishing mechanistic insights and performance benchmarks for bio-based pavement materials. Future studies should investigate long-term durability, oxidative aging, and field-scale validation across diverse climatic and traffic conditions to support broader implementation.

## 5. Declarations

### 5.1. Author Contributions

Conceptualization, P.S., S.T., and S.K.; methodology, P.S. and S.T.; software, P.S. and S.T.; validation, S.T., S.K., P.C., A.W., and P.P.; formal analysis, S.T., A.W., and P.P.; investigation, P.S., S.T., S.K., A.W., and P.P.; resources, P.S., S.T., and S.K.; data curation, S.T., A.W., P.P., and C.T.; writing—original draft preparation, P.S. and S.T.; writing—review and editing, S.T., S.K., P.C., A.W., P.P., and C.T.; visualization, S.T. and P.C.; supervision, S.T. and P.C.; project administration, S.T. and P.C.; funding acquisition, S.T. All authors have read and agreed to the published version of the manuscript.

## 5.2. Data Availability Statement

The data presented in this study are available on request from the corresponding author.

## 5.3. Funding

This research was supported by the Fundamental Fund of Khon Kaen University from the National Science, Research and Innovation Fund (NSRF). The authors would also like to acknowledge the ‘Support by Research and Graduate Studies’ program at Khon Kaen University. Thanks are also due to the Yang Na Integrated Learning Center, Khon Kaen University.

## 5.4. Conflicts of Interest

The authors declare no conflict of interest.

## 6. References

- [1] Liu, Y., Su, P., Li, M., You, Z., & Zhao, M. (2020). Review on evolution and evaluation of asphalt pavement structures and materials. *Journal of Traffic and Transportation Engineering (English Edition)*, 7(5), 573–599. doi:10.1016/j.jtte.2020.05.003.
- [2] Zheng, D., Qian, Z., Liu, Y., & Liu, C. (2018). Prediction and sensitivity analysis of long-term skid resistance of epoxy asphalt mixture based on GA-BP neural network. *Construction and Building Materials*, 158, 614–623. doi:10.1016/j.conbuildmat.2017.10.056.
- [3] Zhu, S., Ji, X., Yuan, H., Li, H., & Xu, X. (2023). Long-term skid resistance and prediction model of asphalt pavement by accelerated pavement testing. *Construction and Building Materials*, 375, 131004. doi:10.1016/j.conbuildmat.2023.131004.
- [4] Azahar, N. B. M., Hassan, N. B. A., Jaya, R. P., Kadir, M. A. B. A., Yunus, N. Z. B. M., & Mahmud, M. Z. H. (2016). An overview on natural rubber application for asphalt modification. *International Journal of Agriculture, Forestry and Plantation*, 2, 212–218.
- [5] Cheriet, F., Soudani, K., & Haddadi, S. (2015). Influence of Natural Rubber on Creep Behavior of Bituminous Concrete. *Procedia - Social and Behavioral Sciences*, 195, 2769–2776. doi:10.1016/j.sbspro.2015.06.391.
- [6] Lo Presti, D. (2013). Recycled Tyre Rubber Modified Bitumens for road asphalt mixtures: A literature review. *Construction and Building Materials*, 49, 863–881. doi:10.1016/j.conbuildmat.2013.09.007.
- [7] Poovaneshvaran, S., Mohd Hasan, M. R., & Putra Jaya, R. (2020). Impacts of recycled crumb rubber powder and natural rubber latex on the modified asphalt rheological behaviour, bonding, and resistance to shear. *Construction and Building Materials*, 234, 117357. doi:10.1016/j.conbuildmat.2019.117357.
- [8] Rodríguez-Fernández, I., Tarpoudi Baheri, F., Cavalli, M. C., Poulikakos, L. D., & Bueno, M. (2020). Microstructure analysis and mechanical performance of crumb rubber modified asphalt concrete using the dry process. *Construction and Building Materials*, 259, 119662. doi:10.1016/j.conbuildmat.2020.119662.
- [9] Gao, J., Wang, H., You, Z., Hasan, M. R. M., Lei, Y., & Irfan, M. (2018). Rheological behavior and sensitivity of wood-derived bio-oil modified asphalt binders. *Applied Sciences (Switzerland)*, 8(6). doi:10.3390/app8060919.
- [10] Alzgool, H. A., Shawashreh, A. M., Albtoosh, L. A., & Abusamra, B. A. (2024). Experimental investigations: Reinforced Concrete Beams Bending Strength with Brine Wastewater in Short Age. *Civil Engineering Journal*, 10(1), 159–170. doi:10.28991/CEJ-2024-010-01-010.
- [11] Rahmawati, C., Aisyah, S., Sanusi, Iqbal, Maulana, M. M., Erdiwansyah, & Ahmad, J. (2024). Artificial Intelligence Models for Predicting the Compressive Strength of Geopolymer Cements. *Civil Engineering Journal*, 10, 37–50. doi:10.28991/CEJ-SP2024-010-03.
- [12] Sani, A., Mohd Hasan, M. R., Shariff, K. A., Jamshidi, A., Ibrahim, A. H., & Poovaneshvaran, S. (2020). Engineering and microscopic characteristics of natural rubber latex modified binders incorporating silane additive. *International Journal of Pavement Engineering*, 21(14), 1874–1883. doi:10.1080/10298436.2019.1573319.
- [13] Saowapark, W., Jubsilp, C., & Rimdusit, S. (2017). Natural rubber latex-modified asphalts for pavement application: effects of phosphoric acid and sulphur addition. *Road Materials and Pavement Design*, 20(1), 211–224. doi:10.1080/14680629.2017.1378117.
- [14] Ansari, A. H., Jakarni, F. M., Muniandy, R., Hassim, S., & Elahi, Z. (2021). Natural rubber as a renewable and sustainable bio-modifier for pavement applications: A review. *Journal of Cleaner Production*, 289. doi:10.1016/j.jclepro.2020.125727.
- [15] Jitsangiam, P., Nusit, K., Phenrat, T., Kumlai, S., & Pra-ai, S. (2021). An examination of natural rubber modified asphalt: Effects of rubber latex contents based on macro- and micro-observation analyses. *Construction and Building Materials*, 289, 123158. doi:10.1016/j.conbuildmat.2021.123158.

- [16] Wititanapanit, J., Carvajal-Munoz, J. S., & Airey, G. (2021). Performance-related and rheological characterisation of natural rubber modified bitumen. *Construction and Building Materials*, 268, 121058. doi:10.1016/j.conbuildmat.2020.121058.
- [17] Gong, J., Han, X., Su, W., Xi, Z., Cai, J., Wang, Q., Li, J., & Xie, H. (2020). Laboratory evaluation of warm-mix epoxy SBS modified asphalt binders containing Sasobit. *Journal of Building Engineering*, 32, 101550. doi:10.1016/j.job.2020.101550.
- [18] Hazoor Ansari, A., Jakarni, F. M., Muniandy, R., Hassim, S., Elahi, Z., & Meftah Ben Zair, M. (2022). Effect of cup lump rubber as a sustainable bio-modifier on the properties of bitumen incorporating polyphosphoric acid. *Construction and Building Materials*, 323, 126505. doi:10.1016/j.conbuildmat.2022.126505.
- [19] Zahoor, M., Nizamuddin, S., Madapusi, S., & Giustozzi, F. (2021). Sustainable asphalt rejuvenation using waste cooking oil: A comprehensive review. *Journal of Cleaner Production*, 278. doi:10.1016/j.jclepro.2020.123304.
- [20] Zargar, M., Ahmadinia, E., Asli, H., & Karim, M. R. (2012). Investigation of the possibility of using waste cooking oil as a rejuvenating agent for aged bitumen. *Journal of Hazardous Materials*, 233–234, 254–258. doi:10.1016/j.jhazmat.2012.06.021.
- [21] Azahar, W. N. A. W., Jaya, R. P., Hainin, M. R., Bujang, M., & Ngadi, N. (2017). Mechanical performance of asphaltic concrete incorporating untreated and treated waste cooking oil. *Construction and Building Materials*, 150, 653–663. doi:10.1016/j.conbuildmat.2017.06.048.
- [22] Ingrassia, L. P., Lu, X., Ferrotti, G., & Canestrari, F. (2019). Chemical and rheological investigation on the short- and long-term aging properties of bio-binders for road pavements. *Construction and Building Materials*, 217, 518–529. doi:10.1016/j.conbuildmat.2019.05.103.
- [23] Zhang, R., Ji, J., You, Z., & Wang, H. (2020). Modification Mechanism of Using Waste Wood-Based Bio-Oil to Modify Petroleum Asphalt. *Journal of Materials in Civil Engineering*, 32(12), 625–634. doi:10.1061/(asce)mt.1943-5533.0003464.
- [24] Hariadi, D., Saleh, S. M., Anwar Yamin, R., & Aprilia, S. (2021). Utilization of LDPE plastic waste on the quality of pyrolysis oil as an asphalt solvent alternative. *Thermal Science and Engineering Progress*, 23. doi:10.1016/j.tsep.2021.100872.
- [25] Kumar, A., & Choudhary, R. (2024). Multiscale evaluation of aging susceptibility of asphalt binders modified with recycled rubber and plastic pyrolytic oil composites. *Construction and Building Materials*, 440, 137473. doi:10.1016/j.conbuildmat.2024.137473.
- [26] Somé, S. C., Pavoine, A., & Chailleux, E. (2016). Evaluation of the potential use of waste sunflower and rapeseed oils-modified natural bitumen as binders for asphalt pavement design. *International Journal of Pavement Research and Technology*, 9(5), 368–375. doi:10.1016/j.ijprt.2016.09.001.
- [27] Zhang, R., Shi, Q., Hu, P., Ji, J., & Suo, Z. (2023). Influence of castor oil-based bio-oil on the properties and microstructure of asphalt binder. *Construction and Building Materials*, 408, 133564. doi:10.1016/j.conbuildmat.2023.133564.
- [28] Ding, Y., Shan, B., Cao, X., Liu, Y., Huang, M., & Tang, B. (2021). Development of bio oil and bio asphalt by hydrothermal liquefaction using lignocellulose. *Journal of Cleaner Production*, 288, 125586. doi:10.1016/j.jclepro.2020.125586.
- [29] Rohayzi, N. F., Katman, H. Y. B., Ibrahim, M. R., Norhisham, S., & Rahman, N. A. (2023). Potential Additives in Natural Rubber-Modified Bitumen: A Review. *Polymers*, 15(8), 1951. doi:10.3390/polym15081951.
- [30] Zhao, X., Li, F., Zhang, X., Cao, J., & Wang, X. (2023). Rheological properties and viscosity reduction mechanism of aromatic/naphthenic oil pre-swelling crumb rubber modified asphalt. *Construction and Building Materials*, 398, 132545. doi:10.1016/j.conbuildmat.2023.132545.
- [31] Zhou, T., Wan, S., & Dong, Z. (2024). Changes in rheological and low-temperature characteristics of rubberized asphalt containing castor-based bio-oil under thermal-oxidative exposure. *Construction and Building Materials*, 411. doi:10.1016/j.conbuildmat.2023.134503.
- [32] Dong, Z., Jiao, Z., Zhou, T., Luan, H., Williams, R. C., Wang, P., & Leng, Z. (2019). Composite modification mechanism of blended bio-asphalt combining styrene-butadiene-styrene with crumb rubber: A sustainable and environmental-friendly solution for wastes. *Journal of Cleaner Production*, 214, 593–605. doi:10.1016/j.jclepro.2019.01.004.
- [33] Ju, Z., Ge, D., Wu, Z., Xue, Y., Lv, S., Li, Y., & Fan, X. (2022). The performance evaluation of high content bio-asphalt modified with polyphosphoric acid. *Construction and Building Materials*, 361. doi:10.1016/j.conbuildmat.2022.129593.
- [34] Zhou, J., Dong, Z., Cao, L., Li, L., Yu, Y., Sun, Z., Zhou, T., & Chen, Z. (2024). Rheological evaluation of paving asphalt binder containing bio-oil from rice straw pyrolysis. *Case Studies in Construction Materials*, 20. doi:10.1016/j.cscm.2024.e03202.
- [35] Kumar, A., & Choudhary, R. (2024). Effect of microwave pretreatment on characteristics of asphalt binders modified with scrap non-tire automotive rubber and waste derived pyrolytic oils after prolonged thermal storage. *Construction and Building Materials*, 419. doi:10.1016/j.conbuildmat.2024.135558.
- [36] Poojeera, S., Benjapiyaporn, C., Intravised, K., Katekaew, S., Senawong, K., & Suiyay, C. (2020). Performance and emission characteristics of the diesel engine fueled by Yang oleoresin blended diesel fuel. *Energy Sources, Part A: Recovery, Utilization, and Environmental Effects*, 46(1), 16318–16335. doi:10.1080/15567036.2020.1817183.

- [37] Suiyay, C., Sudajan, S., Katekaew, S., Senawong, K., & Laloan, K. (2019). Production of gasoline-like-fuel and diesel-like-fuel from hard-resin of Yang (*Dipterocarpus alatus*) using a fast pyrolysis process. *Energy*, 187, 115967. doi:10.1016/j.energy.2019.115967.
- [38] Roschat, W., Phewphong, S., Inthachai, S., Donpamee, K., Phudeetip, N., Leelatam, T., Moonsin, P., Katekaew, S., Namwongsa, K., Yoosuk, B., Janetaisong, P., & Promarak, V. (2024). A highly efficient and cost-effective liquid biofuel for agricultural diesel engines from ternary blending of distilled Yang-Na (*Dipterocarpus alatus*) oil, waste cooking oil biodiesel, and petroleum diesel oil. *Renewable Energy Focus*, 48, 100540. doi:10.1016/j.ref.2024.100540.
- [39] Katekaew, S., Suiyay, C., Senawong, K., Seithtanabutara, V., Intravised, K., & Laloan, K. (2021). Optimization of performance and exhaust emissions of single-cylinder diesel engines fueled by blending diesel-like fuel from Yang-hard resin with waste cooking oil biodiesel via response surface methodology. *Fuel*, 304, 121434. doi:10.1016/j.fuel.2021.121434.
- [40] Sakkampang, C., Kunanon, K., Suwunnasopha, P., & Poojeera, S. (2023). Performance, exhaust emission, and wear behavior of a direct-injection engine using biodiesel from Yang-Na (*Dipterocarpus Alatus*) oleoresins. *Case Studies in Chemical and Environmental Engineering*, 7, 100328. doi:10.1016/j.cscee.2023.100328.
- [41] Suiyay, C., Laloan, K., Katekaew, S., Senawong, K., Noisuwan, P., & Sudajan, S. (2020). Effect of gasoline-like fuel obtained from hard-resin of Yang (*Dipterocarpus alatus*) on single cylinder gasoline engine performance and exhaust emissions. *Renewable Energy*, 153, 634–645. doi:10.1016/j.renene.2020.02.036.
- [42] Daodee, S., Monthakantirat, O., Ruengwinitwong, K., Gatenakorn, K., Maneenet, J., Khamphukdee, C., Sekeroglu, N., Chulikhit, Y., & Kijjoa, A. (2019). Effects of the Ethanol Extract of *Dipterocarpus alatus* Leaf on the Unpredictable Chronic Mild Stress-Induced Depression in ICR Mice and Its Possible Mechanism of Action. *Molecules*, 24(18), 3396. doi:10.3390/molecules24183396.
- [43] Puthongking, P., Yongram, C., Katekaew, S., Sungthong, B., & Weerapreeyakul, N. (2022). *Dipterocarpol* in Oleoresin of *Dipterocarpus alatus* Attributed to Cytotoxicity and Apoptosis-Inducing Effect. *Molecules*, 27(10), 3187. doi:10.3390/molecules27103187.
- [44] TIS 851-2018. (2018). Asphalt cement for use in pavement construction. Thai Industrial Standard Institute, Bangkok, Thailand. (In Thai).
- [45] DH-SP 409-2013. (2013). Specification for Natural Rubber Modified Asphalt. Department of Highways, Bangkok, Thailand. (In Thai).
- [46] ASTM D5/D5M-13. (2019). Standard Test Method for Penetration of Bituminous Materials. ASTM International, Pennsylvania, United States. doi:10.1520/D0005\_D0005M-13.
- [47] ASTM D113-17. (2023). Standard Test Method for Ductility of Asphalt Materials. ASTM International, Pennsylvania, United States. doi:10.1520/D0113-17.
- [48] ASTM D36-06. (2010). Standard Test Method for Softening Point of Bitumen (Ring-and-Ball Apparatus). ASTM International, Pennsylvania, United States. doi:10.1520/D0036-06.
- [49] ASTM D4402/D4402M-23. (2023). Standard Test Method for Viscosity Determination of Asphalt at Elevated Temperatures Using a Rotational Viscometer. ASTM International, Pennsylvania, United States. doi:10.1520/D4402\_D4402M-23.
- [50] ASTM D7175-23. (1995). Standard Test Method for Determining the Rheological Properties of Asphalt Binder Using a Dynamic Shear Rheometer. ASTM International, Pennsylvania, United States. doi:10.1520/D7175-23.
- [51] ASTM D6927-22. (2022). Standard Test Method for Marshall Stability and Flow of Asphalt Mixtures. ASTM International, Pennsylvania, United States. doi:10.1520/D6927-22.
- [52] DH-S 408/2532. (1989). Asphalt concrete or Hot-Mix asphalt. Department of Highways, Bangkok, Thailand. (In Thai).
- [53] Tuntiworawit, N., Lavansiri, D., & Phromsorn, C. (2005). The Modification of Asphalt with Natural Rubber Latex. *Proceedings of the Eastern Asia Society for Transportation Studies*, 5, 679–694.
- [54] Al-Mansob, R. A., Ismail, A., Alduri, A. N., Azhari, C. H., Karim, M. R., & Yusoff, N. I. M. (2014). Physical and rheological properties of epoxidized natural rubber modified bitumens. *Construction and Building Materials*, 63, 242–248. doi:10.1016/j.conbuildmat.2014.04.026.
- [55] Siddiqui, M. N., Ali, M. F., & Shirokoff, J. (2002). Use of X-ray diffraction in assessing the aging pattern of asphalt fractions. *Fuel*, 81(1), 51–58. doi:10.1016/S0016-2361(01)00116-8.
- [56] Phetcharaburanin, J., Deewai, S., Kulhawatsiri, T., Moolpia, K., Suksawat, M., Promraksa, B., Klanrit, P., Namwat, N., Loilome, W., Poopasit, K., Katekaew, S., & Phetcharaburanin, P. (2020). 1H NMR metabolic phenotyping of *Dipterocarpus alatus* as a novel tool for age and growth determination. *PLOS ONE*, 15(12), e0243432. doi:10.1371/journal.pone.0243432.